OPEN

Correspondence and
requests for materials
should be addressed to
T.A. (taro@crl.hpk.co.
jp)

* These authors
contributed equally to
this work.

Direct evidence for three-dimensional off-axis trapping with single Laguerre-Gaussian beam

T. Otsu[1]*, T. Ando[1]*, Y. Takiguchi[1], Y. Ohtake[1], H. Toyoda[1] & H. Itoh[2]

[1]Central Research Laboratory, Hamamatsu Photonics K.K., Hirakuchi, Hamakita-ku, Hamamatsu 434-8601, Japan, [2]Tsukuba Research Laboratory, Hamamatsu Photonics K.K., Tokodai, Tsukuba 300-2635, Japan.

Optical tweezers are often applied to control the dynamics of objects by scanning light. However, there is a limitation that objects fail to track the scan when the drag exceeds the trapping force. In contrast, Laguerre-Gaussian (LG) beams can directly control the torque on objects and provide a typical model for nonequilibrium systems such as Brownian motion under external fields. Although stable "mid-water" trapping is essential for removing extrinsic hydrodynamic effects in such studies, three-dimensional trapping by LG beams has not yet been clearly established. Here we report the three-dimensional off-axis trapping of dielectric spheres using high-quality LG beams generated by a special holographic method. The trapping position was estimated as ∼ half the wavelength behind the beam waist. These results establish the scientific groundwork of LG trapping and the technical basis of calibrating optical torque to provide powerful tools for studying energy-conversion mechanisms and the nonequilibrium nature of biological molecules under torque.

O ptical tweezers have become essential tools for the experimental study of single-molecule biophysics[1-3] and nonequilibrium statistical physics[4-7] due to the controllability of the pico-Newton force with nano-metre-scale position precision. The basic function of optical tweezers is to trap dielectric objects in three-dimensional space where the scattering and gradient forces of light are balanced. This mechanism is often called gradient-force trapping[8,9]. It is also possible to control the dynamics of trapped objects by scanning light[4-7]; however, this approach is not directly applicable to the object's motion. The trapped object fails to track the scan when the viscous drag exceeds the trapping force for extremely quick scans. Another way of controlling dynamics is to introduce force fields, e.g. optical vortices (OV)[10-18], which have the special property of carrying orbital angular momenta, can produce nearly ideal torque fields producing endless revolutions of dielectric objects[19-23]. Optical tweezers with OV are expected to provide powerful tools for the experimental studies of nonequilibrium statistical mechanics[24], e.g. nonadiabatic transitions among nonequilibrium stationary states[25].

Since the principle of gradient-force trapping is simple and universal, compatibility between optical tweezers and OV appears straightforward. This impression, however, might introduce confusion to a general description of optical trapping by OV. The term "trapping", which Ashkin introduced to indicate the three-dimensional version for Gaussian trapping[8,9], is now overused for the two-dimensional case in OV trapping[14,15,21,22,26]. So far, experimental studies of three-dimensional OV trapping have been reported in the context of equivalence between the spin and orbital angular momenta of Laguerre-Gaussian (LG) beams[10-13], which have received general attention for the past two decades as a series of the most common and natural embodiments of OV as well as the fundamental elements of light propagation[16]. In these experimental reports, the transversal properties of LG trapping were studied by observing objects rotating around their own axes at the beam centre, but the axial trapping property failed to be firmly established. The properties of LG trapping have also been discussed from a theoretical point of view by several groups[21,27-32] in relation to the detailed study of light's scattering force. Nevertheless, the situation resembles that in the experimental studies except that a few studies discussed the axial stability of LG trapping[27,29,32] in on-axis trapping.

The axial property of LG trapping becomes more obscure in the case of off-axis trapping. It is also experimentally difficult to achieve three-dimensional off-axis trapping by only a single LG beam of micrometre-sized dielectric objects. One reason for the difficulty is that the gradient force in LG trapping tends to become smaller than the usual Gaussian trapping due to the lower spatial concentration of the light-power distribution for LG beams. Moreover, a common phase–only-modulation holographic method for generating LG beams further
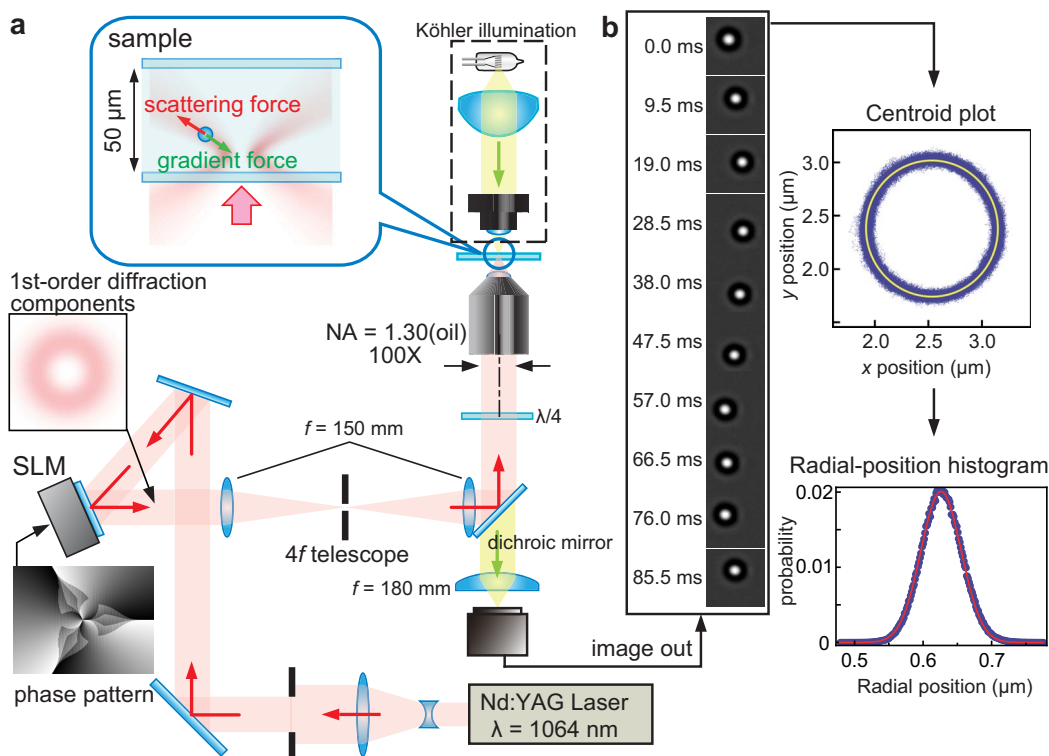
Figure 1 | Outlines of experiments and analysis. (a) Optical system. Blue inset shows schematic picture of a submicrometre-sized polystyrene sphere trapped by balance between scattering and gradient forces of a LG beam. (b) Data processing flow for deriving a revolution radius from series of sphere images. Images of revolving polystyrene spheres were converted to a time series of centroid information. Centre of revolution was first determined by fitting a series of centroid data to a circular orbit. Then the radial-position distribution was obtained with respect to the centre, and R_s was derived by fitting the radial distribution to a Gaussian profile.

reduces the axial light-power concentration because of the mixture of radially higher-order LG-mode contents[33]. Radially higher-order LG modes have multi-ringed patterns, where the inner rings are enlarged in the axial direction to produce smaller axial gradient forces than the lower-order modes. As a result, such additional tricks as gravity[19], the surface of a cover glass[21,22,26], and another Gaussian trapping beam[34] are necessary to fix the axial trapping position in the LG trapping. On the other hand, the off-axis revolution of small dielectric objects on a three-dimensional circular trajectory has recently been achieved[35–37] by introducing another optical technique. However, this technique depends on artificial optical fields specific to the three-dimensional revolution, and a fundamental question in optical science remains: can a single pure LG beam achieve three-dimensional off-axis trapping of small dielectric objects?

This paper reports the stable off-axis trapping of micrometre-sized dielectric spheres using holographically generated high-quality LG beams under microscopy. A holographic complex-amplitude modulation scheme[33] was introduced to generate various LG beams of mode purities over 95%[38]. This approach enabled three-dimensional trapping with sufficient trapping stability for quantitative study. Evidence of three-dimensional LG trapping was also established by observing the revolutions of micrometre-sized dielectric spheres trapped in "mid-water", i.e., completely surrounded by water, not touching the bottom or any wall of the chamber. We confirmed three-dimensional LG trapping without any LG-independent supports due the revolution radius of a dielectric sphere trapped in a 50-μm-thick water layer being independent of the LG-beam power. Moreover, the axial trapping position was estimated to be $\sim$ half wavelength behind the beam waist from the changes in the revolution radii; these changes were caused mechanically by pressing the revolving spheres onto a pair of glass walls separated by 3 μm. From another viewpoint, the hydrodynamic surface coupling effect of

viscous drag on the trapped sphere was also simultaneously evaluated to confirm the trapping in mid-water.

Since the forces applied to objects are usually derived according to the viscous drag of the surrounding medium in microscopy, stable three-dimensional LG trapping is essential for determining the absolute optical torque free from surface effects on viscous drag[39,40] and for establishing the technical grounds of optical tweezers as manipulation tools in the microscopy world. Optical tweezers with LG beams are also expected to enhance progress in such fields as the torsional properties of biological molecules[41,42], microrheology[39,40], and nonequilibrium statistical mechanics[4–7,43,44].

In the following, we restrict our interest to the radially lowest-order LG beams that present single-ringed doughnut patterns and carry the orbital angular momenta of $l\hbar$ per photon, where l is an integer number referred to as an azimuthal-mode index. A dielectric object irradiated by light receives a total force equal to the sum of the scattering and gradient forces acting on each small portion of the object[45]. Following this simple picture, higher-index dielectric objects under the irradiation of an LG beam are expected to be revolved on the ring pattern by being trapped on a plane slightly behind the beam waist, where the scattering and gradient forces are balanced (blue-lined inset in Fig. 1a).

Results

Dependence of revolution radius on LG-beam power. To confirm that micrometre-sized dielectric objects can be trapped in mid-water on the bright rings of LG beams without any light-independent support, we first examined the behaviour of the revolution radius (R_s) against incident LG-beam power (P_{LG}) under the condition where a glass surface lies too far from the trapped objects to support trapping. Since LG beams keep similar beam patterns of different sizes during propagation[16], the cross-sectional light-power
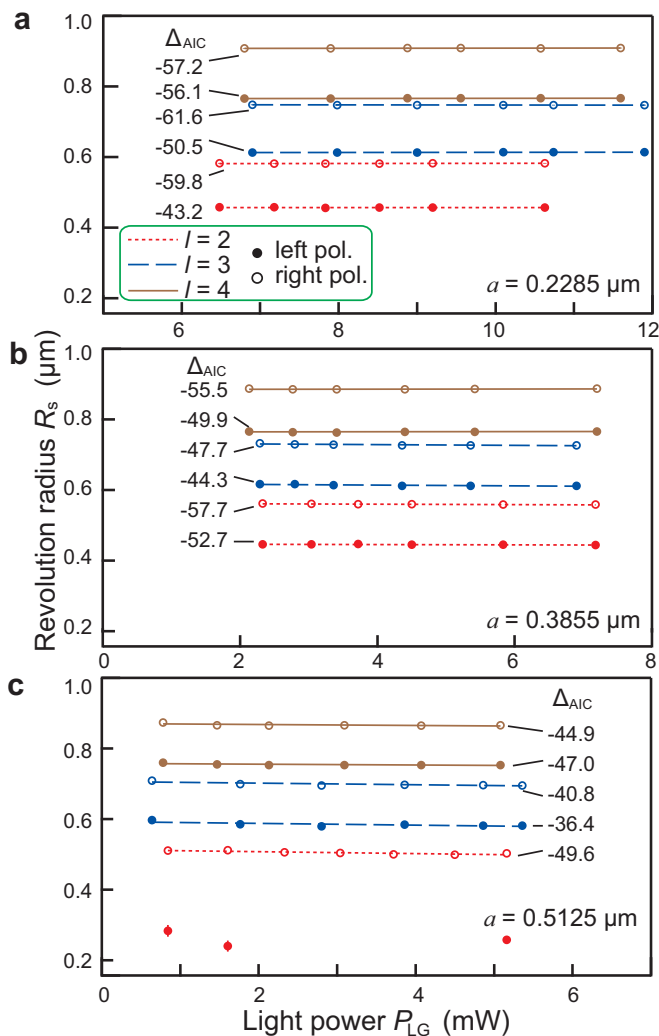
Figure 2 | Behaviour of revolution radius under change of light power for polystyrene spheres of various radii. (a), (b), and (c) show experimental results for polystyrene spheres of radius 0.2285, 0.3855, and 0.51255 μm, respectively. Errors in revolution radii are evaluated as standard deviations of ten measurements but five times smaller than plot symbols. In each figure, classifications of trapping LG beams are distinguished by different colours and symbols: red, blue, and brown represent $l = 2$, 3, and 4, respectively, and closed and open circles denote left and right polarizations. Straight lines show most suitable linear models for the light-power dependence of the revolution radius under individual conditions of trapping LG beam and sphere radius. Each value denoted as Δ_{AIC} is a result of the subtraction of AIC for a square-root model from that for a linear model, providing a benchmark for the goodness of the linear model.

density should be inversely proportional to the square of the beam radius. We start by considering a situation where a dielectric sphere was trapped by the balance between the scattering and other light-independent forces (e.g., gravity) at P_{LG}. When P_{LG} is increased α times, the balance position will shift to where the light-power density is about α^{-1} times, because the total scattering force is approximately proportional to an integral of the light-power density over the spherical volume. According to the above mechanism, R_s must be proportional to $P_{LG}^{1/2}$ for trapping with light-independent supports, while R_s is independent of P_{LG} for gradient-force trapping.

Figures 1a and 1b show schematic pictures of the setup and the procedure for observing the motions of polystyrene spheres trapped in mid-water by holographically generated LG beams[33] (See Methods). The changes in R_s versus P_{LG} were measured for various

conditions that were determined as combinations of three different sphere sizes, polarizations, and azimuthal-mode index l of the LG beams. Here, the values of P_{LG} were measured in advance at the sample position under dry conditions. Figures 2a–2c exhibit the change of R_s against P_{LG}, where the R_s values agree with the effects of polarization and l on the bright-ring radius of LG beams under tight-focusing conditions[46]. The revolutions were highly stable and uniform around the bright ring of the LG beams, and all plot symbols in Figs. 2a–2c cover intervals of over five times the standard deviation of measured R_s, except the case of trapping by the left-polarized $l = 2$ LG beam in Fig. 2c, which became unstable and the standard deviation became comparable to the plot symbols.

In contrast, trapping of the 0.5125-μm-radius beads by the left-polarized $l = 2$ LG beam belonged to an on-axis trapping condition, where the size of the trapped object exceeded the diameter of the trapping LG beam. The stability of on-axis trapping was discussed in detail from the viewpoint of deterministic dynamics in Ref. 32 and assigned to the competition between the dynamics and the damping. In fact, R_s was not always determined as a well-defined value or it became anomalously small compared to that for stable trapping even if it were successfully determined, indicating the instability of on-axis trapping. On-axis trapping phenomena also suffer from thermal fluctuations presenting more complicated dynamics, which is beyond the scope of the present study but an interesting topic for future study.

We compared the goodness of the linear and square-root models for the P_{LG}-dependence of the R_s in the context of Akaike's information criterion (AIC) that enables comparisons between two models of different degrees of freedom. Although small but meaningful negative inclinations were observed in the fitted linear models, the AICs for the linear models are at least 36.4 smaller than those for the square-root models. Such differences in AIC over $10\times$ of the model's degree of freedom indicate that the behaviour of R_s almost completely mismatches the assumption of dominant light-independent forces.

Estimation of trapping position. We establish direct evidence of LG-beam trapping in mid-water by estimating the axial trapping position with an approach that is effective even in regimes smaller than the wavelength of light. A focused LG beam, whose behaviour resembles a Gaussian beam, shrinks toward the beam waist during propagation (we assume the propagation into the z direction) and diverges after passing the beam waist position. Using this property, the axial trapping position can be estimated by the following idea (Figs. 3a–3c). We start from a situation where a polystyrene sphere of radius a is trapped in mid-water under the balance between the gradient and scattering forces as in Fig. 1a. In this situation, the sphere revolves on the bright ring of the LG beam at trapping position z_t (dashed line in Fig. 3b). Here, the trapping position indicates a relative position in the sample, although z_t should almost be fixed during the mid-water trapping if measured from the beam waist. When the sample is scanned toward the z-direction and the sphere reaches the front cover glass (Fig. 3a), R_s will increase while keeping the trapping position z_1 during the "forward" scan. In contrast, when the sample is scanned against the z-direction and the sphere reaches the backward cover glass (Fig. 3c), the trapping position becomes fixed at z_2. In this situation, R_s decreases as the trapping position approaches the beam waist and starts increasing after passing over the minimum radius. Following the above mechanism, we obtain an R_s profile if R_s is measured along with a continuous scan.

The trapping position was estimated by using a 3-μm-thick flow cell (See Methods). We fixed the polarization of the incident LG beams to the right polarization to suppress the relative errors in R_s and chose P_{LG} as 4.15, 4.38, and 4.00 mW for $l = 2$, 3, and 4 LG beams, respectively, to perform experiments under stable revolution.
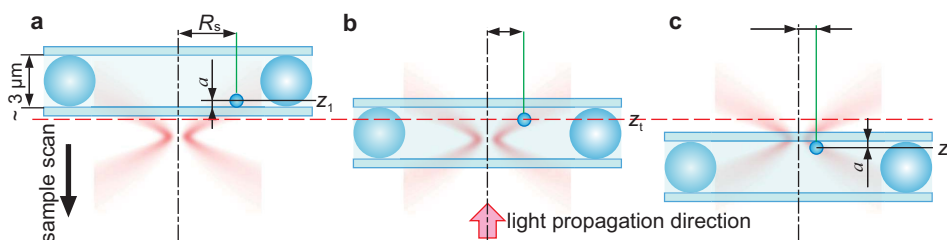
Figure 3 | Schematic picture of estimating revolution radius by sample scan. Three different situations in sample scan: (a) two-dimensional trapping on front interface, (b) three-dimensional trapping free from interfaces, and (c) two-dimensional trapping on back interface. Here, z_1 indicates the position behind the front glass surface by distance a, and z_2 indicates the position in front of the backward glass surface by a.

Figures 4a–4c show the changes in the measured values according to the relative z-position of the sample (in optical length: i.e., scanning distance from the minimum R_s position multiplied by the refractive index of water) for LG beams of $l = 2, 3,$ and 4. Here, red plots show the R_s with horizontal and vertical errors, where the horizontal errors are determined as a fifth of the minimum scale of the micrometre for sample scanning and the vertical errors are derived in a similar way as for the case of Figs. 2a–2c. The R_s profiles match the predictions from the above "pressing scheme". The plateaus in the R_s profile indicate trapping in the mid-water, and the plateau widths are commonly consistent with $|z_2 - z_1|$ ($= 2.348 \pm 0.166$ μm from the sample specifications).

We also evaluated the viscous drag imposed on a revolving sphere in each condition to estimate the hydrodynamic coupling effect with glass surfaces in terms of Faxén's correction[40], which appears to enhance the viscous drag coefficient around the surfaces (See Supplementary Information). The blue plots in Figs. 4a–4c show the changes in the viscous drag coefficient that were derived from the correlation analyses on the azimuthal dynamics of the dielectric spheres. In fact, the small viscous drag domains are consistent with the plateaus in the R_s profile, which also supports the trapping in mid-water between the glass surfaces. Following the pressing scheme, the trapping position roughly corresponds to the "backward" edge of the plateau, which is commonly about 0.6 times the light wavelength behind the beam waist for $l = 2, 3,$ and 4. Although this is not a quantitative estimation for the trapping position, it is nevertheless the first direct evidence for three-dimensional off-axis trapping with LG beams.

Discussion

In the present study, we estimated the trapping position by scanning the samples in the propagation direction of the trapping LG beams. Although the scan range was at most a few wavelengths, this can change the incident optical condition of the LG beams to the glass/water interface. For example, subtle inclinations are observed at the plateaus of R_s in Figs. 4a–4c, which can arise from the scanning effect. Nevertheless, we recognise it as minor in the present results because the LG-beam shapes around the beam waists are reproduced in Figs. 4a–4c. This means that the present scanning scheme is also effective for roughly observing the propagation behaviour of the LG beams under tightly-focused conditions. Even though the heat transfer from the trapping LG beams to the sample is also supposed to affect the refractive index of water[47], the change is estimated to be $\sim -0.01\%/°C$, which will produce only minor optical effects.

On the other hand, the viscous drag coefficients in Figs. 4a–4c present odd behaviour in the $z > 0$ domain, although the viscosity is expected to increase monotonously here. The main origin of this phenomenon might be the LG beams reflected from the backward glass surface. In the $z > 0$ domain, the dielectric spheres usually revolve around the backward surface (Fig. 3c) and suffer from the effects of the reflected LG beams. The scattering force of the reflected light reduces the total force that presses the spheres onto the glass
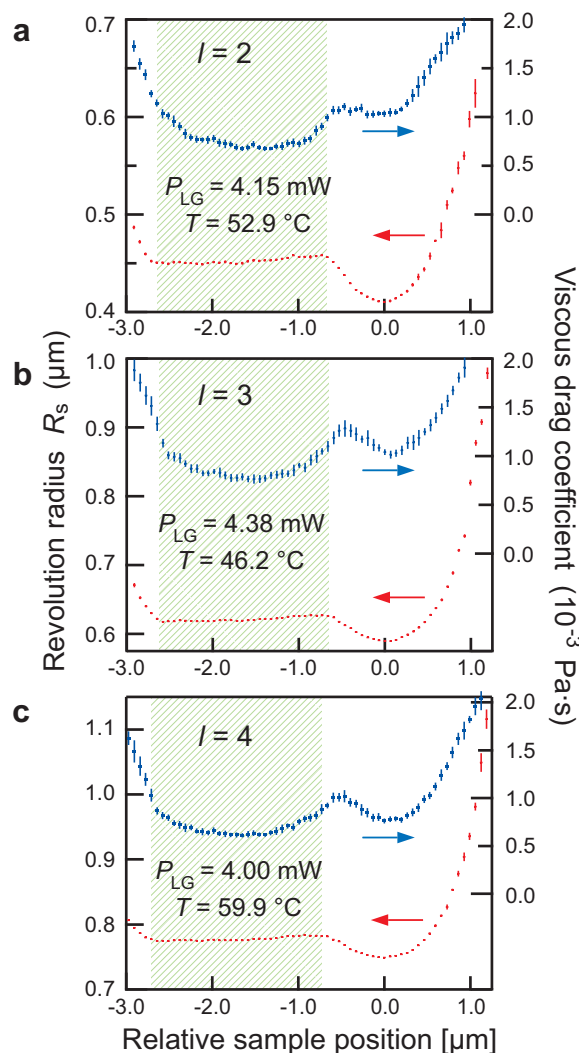

Figure 4 | Revolution radius and viscosity versus sample position. Behaviour of revolution radius (red plots: labeled on left axis) and viscous drag coefficient (blue plots: labeled on right axis) are shown as functions of sample position for (a) $l = 2$, (b) $l = 3$, and (c) $l = 4$ LG beams. Here, vertical error bars indicate standard deviations of ten measured values. Each sample position in horizontal axis is as sample-scan distance measured from "beam waist" position (sample position marking minimum revolution radius) in optical length, i.e., relative scan distance multiplied by the refractive index of water. The error in sample position is determined as a fifth of the minimum scale of micrometre for sample scanning. Hatched areas indicate mid-water trapping regimes corresponding to situation of Fig. 3b to guide the eyes for comparing behaviours of revolution radius and viscous drag.

surface, and they can move away from the surface to present a superficial decrease of Faxén's correction on the viscous drag coefficient. This hypothesis also matches the absence of similar behaviour in $z < -2.5\lambda$, where the objects are likely to revolve around the front glass surface and the effects of the reflected LG beams are ignored.

The present setup, which essentially combines a high-speed CMOS image sensor and a computer-controllable spatial light modulator (SLM), is expected to provide a powerful tool for the experimental study of nonequilibrium statistical mechanics. In particular, the study of the information-to-heat conversion[43,44], which requires the detection of an object's position and the switching of a force field based on the observed position information in the millisecond regime, is further developed by the present experimental technology, if the response time of SLM devices is further improved.

Methods

Samples. We suspended three sizes of polystyrene spheres (Polysciences Inc., Polybead® Cat# 07310, Cat# 07309, and Cat# 07307, diameters 1.025 ± 0.010, 0.771 ± 0.024, and 0.457 ± 0.011 μm, respectively) in ultra pure water (MilliQ) and put between 24 × 40 and 18 × 18 mm² cover glasses (NEO, Matsunami: No. 1) with 50-μm-thick spacers. The edges of the smaller cover glasses were sealed with resin to make flow cells for the measurements of R_s versus various P_{LG}. For the trapping-position estimation, Cat# 07309 polystyrene spheres were infused with a few 3-μm-diameter spheres (Polybead® Cat# 17134: diameter 3.119 ± 0.164 μm) that will eventually become spacers.

Optical setup. LG beams were generated from linearly polarized laser light (Millennia® IR, Spectra Physics; wavelength $\lambda = 1,064$ nm) as first-order diffraction components from holograms displayed on an SLM (X10468, Hamamatsu Photonics). The generated LG beams were introduced to an inverted microscope (IX71, Olympus) equipped with a stable mechanical stage (KS-O, Chuukousya Seisakujo) and focused on samples through an oil-immersion objective (UPLFLN 100X UIS2, numerical aperture 1.30, Olympus) after being converted to circular polarization with a quarter-wave plate. The visible images of the polystyrene spheres were observed by a high-speed CMOS image sensor (C8201, Hamamatsu Photonics), which can acquire and process 6,337 images per second at the cost of a limited active area (64 × 64 pixels, each of which covers a 0.1 × 0.1 μm² area on the observing plane). The image sensor was mounted on a position-adjustment rail to observe the images under off-focus conditions. Trapping positions were estimated by scanning the sample stage in one way of the z direction, manually turning a micrometre and adjusting the sensor position. The change in the image magnification due to the sensor-position adjustment was estimated to be less than ±0.25% with a test pattern ruled into 10-μm squares, meaning that errors in R_s are less than statistical deviations. Notice that precise adjustment and selection of the optical elements is essential for trapping with LG beams.

Hologram design. We applied a holographic complex-amplitude modulation method to generate high-quality LG beams[33,38] of arbitrary orders. The holograms were designed by the Kirk-Jones method, and four pixels were chosen for the blazing pitch. The beam-size parameters were determined to obtain LG beams that have a common Gaussian radius of 1.42 mm at the objective's entrance pupil. The holograms were displayed on the SLM after adding a compensation pattern for the optical distortion and a Fresnel lens pattern (radius of curvature = 2,759 mm) for adjusting the focus position of the $\lambda = 1,064$ nm LG beams.

Analysis. Images of the revolving polystyrene spheres were converted to a time series of centroid information. Typically, 40,000 images were captured in a single measurement, and the measurements were repeated ten times under the same conditions to compose a sequence of experiments. The centroids were determined with a position uncertainty less than 0.01 pixels corresponding to 1 nm under the present setup. The revolution's centre was first determined by fitting a series of centroid data to a circular orbit. Then the radial-position distribution was obtained with respect to the centre, and the R_s was derived by fitting the radial distribution to a Gaussian profile (Fig. 1b). Since the fitting errors in R_s were typically 0.1 nm under mid-water trapping conditions, the total errors in R_s were dominated by statistical deviation.

1. Liphardt, J., Dumont, S., Smith, S. B., Tinoco, I. Jr & Bustamante, C. Equilibrium information from nonequilibrium measurements in an experimental test of the Jarzynski equality. *Science* **296**, 1832–1835 (2002).
2. Trepagnier, E. H. *et al.* Experimental test of Hatano and Sasa's nonequilibrium steady-state equality. *Proc. Natl. Acad. Sci. USA* **101**, 15038–15041 (2004).
3. Collin, D. *et al.* Verification of the Crooks fluctuation theorem and recovery of RNA folding free energies. *Nature* **437**, 231–234 (2005).
4. Wang, G. M., Sevick, E. M., Mittag, E., Searles, D. J. & Evans, D. J. Experimental demonstration of violations of the second law of thermodynamics for small systems and short time scales. *Phys. Rev. Lett.* **89**, 050601 (2002).
5. Wang, G. M. *et al.* Experimental study of the fluctuation theorem in a nonequilibrium steady state. *Phys. Rev. E* **71**, 046142 (2005).
6. Toyabe, S., Jiang, H.-R., Nakamura, T., Murayama, Y. & Sano, M. Experimental test of a new equality: Measuring heat dissipation in an optically driven colloidal system. *Phys. Rev. E* **75**, 011122 (2007).
7. Toyabe, S. & Sano, M. Energy dissipation of a Brownian particle in a viscoelastic fluid. *Phys. Rev. E* **77**, 041403 (2008).
8. Ashkin, A., Dziedzic, J. M., Bjorkholm, J. E. & Chu, S. Observation of a single-beam gradient force optical trap for dielectric particles. *Opt. Lett.* **11**, 288–290 (1986).
9. Ashkin, A. Optical trapping and manipulation of neutral particles using lasers. *Proc. Natl. Acad. Sci. USA* **94**, 4853–4860 (1997).
10. He, H., Friese, M. E. J., Heckenberg, N. R. & Rubinstein-Dunlop, H. Direct observation of transfer of angular momentum to absorptive particles from a laser beam with a phase singularity. *Phys. Rev. Lett.* **75**, 826–829 (1995).
11. Friese, M. E. J., Enger, J., Rubinsztein-Dunlop, H. & Heckenberg, N. R. Optical angular-momentum transfer to trapped absorbing particles. *Phys. Rev. A* **54**, 1593–1596 (1996).
12. Simpson, N. B., Dholakia, K., Allen, L. & Padgett, M. J. Mechanical equivalence of spin and orbital angular momentum of light: an optical spanner. *Opt. Lett.* **22**, 52–54 (1997).
13. Friese, M. E. J., Nieminen, T. A., Heckenberg, N. R. & Rubinsztein-Dunlop, H. Optical alignment and spinning of laser-trapping microscopic particles. *Nature* **394**, 348–350 (1998).
14. Volke-Sepulveda, K., Garcés-Chávez, V., Chávez-Cerda, S., Arlt, J. & Dholakia, K. Orbital angular momentum of a high-order Bessel light beam. *J. Opt. B* **4**, S82–S89 (2002).
15. Grier, D. G. A revolution in optical manipulation. *Nature* **424**, 810–816 (2003).
16. Allen, L., Barnett, S. M. & Padgett, M. J. *Optical Angular Momentum* (Institute of Physics Pub., Bristol and Philadelphia, 2003).
17. Grier, D. G. & Roichman, Y. Holographic optical trapping. *Appl. Opt.* **45**, 880–887 (2006).
18. Padgett, M. & Bowman, R. Tweezers with a twist. *Nature Photon.* **5**, 343–348 (2011).
19. O'Neil, A. T. & Padgett, M. J. Three-dimensional optical confinement of micron-sized metal particles and the decoupling of the spin and orbital angular momentum within an optical spanner. *Opt. Commun.* **185**, 139–143 (2000).
20. O'Neil, A. T., MacVicar, I., Allen, L. & Padgett, M. J. Intrinsic and extrinsic nature of the orbital angular momentum of a light beam. *Phys. Rev. Lett.* **88**, 053601 (2002).
21. Garcés-Chávez, V., Volke-Sepulveda, K., Chávez-Cerda, S., Sibbett, W. & Dholakia, K. Transfer of orbital angular momentum to an optically trapped low-index particle. *Phys. Rev. A* **66**, 063402 (2002).
22. Garcés-Chávez, V. *et al.* Observation of transfer of the local angular momentum density of a multiringed light beam to an optically trapped particle. *Phys. Rev. Lett.* **91**, 093602 (2003).
23. Curtis, J. E. & Grier, D. G. Structure of optical vortices. *Phys. Rev. Lett.* **90**, 133901 (2003).
24. Kubo, R., Toda, M. & Hashitsume, N. *Statistical Physics II Nonequilibrium Statistical Mechanics, 2nd. ed.* (Springer-Verlag, Berlin Heidelberg New York, 1991).
25. Seifert, U. Stochastic thermodynamics, fluctuation theorems and molecular machines. *Rep. Prog. Phys.* **75**, 126001 (2012).
26. Chen, M., Mazilu, M., Arita, Y., Wright, E. M. & Dholakia, K. Dynamics of microparticles trapped in a perfect vortex beam. *Opt. Lett.* **38**, 4919–4922 (2013).
27. Gahagan, K. T. & Swartzlander, G. A. Jr Optical vortex trapping of particles. *Opt. Lett.* **21**, 827–829 (1996).
28. Ganic, D., Gan, X. & Gu, M. Optical trapping force with annular and doughnut laser beams based on vectorial diffraction. *Opt. Express* **13**, 1260–1265 (2005).
29. Sun, B., Roichman, Y. & Grier, D. G. Theory of holographic optical trapping. *Opt. Express* **16**, 15765–15776 (2008).
30. Simpson, S. H. & Hanna, S. Optical angular momentum transfer by Laguerre-Gaussian beams. *J. Opt. Soc. Am A* **26**, 625–638 (2009).
31. Simpson, S. H. & Hanna, S. Orbital motion of optically trapped particles in Laguerre-Gaussian beams. *J. Opt. Soc. Am A* **27**, 2061–2071 (2010).
32. Ng, J., Lin, Z. & Chan, C. T. Theory of optical trapping by an optical vortex beam. *Phys. Rev. Lett.* **104**, 103601 (2010).
33. Ando, T., Ohtake, Y., Matsumoto, N., Inoue, T. & Fukuchi, N. Mode purities of Laguerre-Gaussian beams generated via complex-amplitude modulation using phase-only spatial light modulators. *Opt. Lett.* **34**, 34–36 (2009).
34. Volpe, G. & Petrov, D. Torque detection using Brownian fluctuations. *Phys. Rev. Lett.* **97**, 210603 (2006).
35. Roichman, Y. & Grier, D. G. Three-dimensional holographic ring traps. *Proc. SPIE* **6483**, 64830F (2007).
36. Roichman, Y., Sun, B., Roichman, Y., Amato-Grill, J. & Grier, D. G. Optical forces arising from phase gradients. *Phys. Rev. Lett.* **100**, 013602 (2008).
37. Shanblatt, E. R. & Grier, D. G. Extended and knotted optical traps in three dimensions. *Opt. Express* **19**, 5833–5838 (2011).
38. Ando, T., Matsumoto, N., Ohtake, Y., Takiguchi, Y. & Inoue, T. Structure of optical singularities in coaxial superpositions of Laguerre-Gaussian modes. *J. Opt. Soc. Am. A* **27**, 2602–2612 (2010).

39. Bishop, A. I., Nieminen, T. A., Heckenberg, N. R. & Rubinsztein-Dunlop, H. Optical microrheology using rotating laser-trapped particles. *Phys. Rev. Lett.* **92**, 198104 (2004).

40. Leach, J. *et al.* Comparison of Faxén's correction for a microsphere translating or rotating near a surface. *Phys. Rev. E* **79**, 026301 (2009).

41. Itoh, H. *et al.* Mechanically driven ATP synthesis by F1-ATPase. *Nature* **427**, 465–468 (2004).

42. Fazal, F. M. & Block, S. M. Optical tweezers study life under tension. *Nature Photon.* **5**, 318–321 (2011).

43. Toyabe, S., Sagawa, T., Ueda, M., Muneyuki, E. & Sano, M. Experimental demonstration of information-to-energy conversion and validation of the generalized Jarzynski equality. *Nat. Phys.* **6**, 988–992 (2010).

44. Bérut, A. *et al.* Experimental verification of Landauer's principle linking information and thermodynamics. *Nature* **483**, 187–189 (2012).

45. Rohrbach, A. & Stelzer, E. H. K. Optical trapping of dielectric particles in arbitrary fields. *J. Opt. Soc. Am. A* **18**, 839–853 (2001).

46. Iketaki, Y., Watanabe, T., Bokor, N. & Fujii, M. Investigation of the center intensity of first-and second-order Laguerre-Gaussian beams with linear and circular polarization. *Opt. Lett.* **32**, 2357–2359 (2007).

47. Harvey, A. H., Gallagher, J. S. & Levelt Sengers, J. M. H. Revised formulation for the refractive index of water and steam as a function of wavelength, temperature and density. *J. Phys. Chem. Ref. Data* **27**, 761–774 (1998).

Author contributions

T.O. constructed the complete experimental setup and performed the experiments; T.A. designed the present study, performed its data analyses, and wrote the manuscript; Y.T. contributed to the construction of the optical and holographic setups; Y.O. contributed to the data analyses and the manuscript preparation; H.T. coordinated the detection system; H.I. contributed to establishing the conception and design of the study and provided direction for the microscopy.

Additional information

Supplementary information accompanies this paper at http://www.nature.com/scientificreports

Competing financial interests: All authors are employees of Hamamatsu Photonics K.K., Japan.

How to cite this article: Otsu, T. *et al.* Direct evidence for three-dimensional off-axis trapping with single Laguerre-Gaussian beam. *Sci. Rep.* **4**, 4579; DOI:10.1038/srep04579 (2014).